5-oxoETE triggers nociception in constipation-predominant irritable bowel syndrome through MAS-related G protein–coupled receptor D

Tereza Bautzova, James Hockley, Teresa Pérez-Berezo, Julien Pujo, Michael Tranter, Cléo Desormeaux, Maria Raffaella Barbaro, Lilian Basso, Pauline Le Faouder, Corinne Rolland, et al.

Title: 5-oxoETE triggers nociception in constipation predominant irritable bowel syndrome through MAS-related G protein coupled receptor D

Authors: Tereza Bautzova[1]†, James RF Hockley[2,3]†, Teresa Perez-Berezo[1]†, Julien Pujo[1], Michael M Tranter[3], Cleo Desormeaux[1], Maria Raffaella Barbaro[5], Lilian Basso[1#], Pauline Le Faouder[4], Corinne Rolland[1], Pascale Malapert[6], Aziz Moqrich[6], Helene Eutamene[7], Alexandre Denadai-Souza[1], Nathalie Vergnolle[1], Ewan St John Smith[2], David I Hughes[8], Giovanni Barbara[5], Gilles Dietrich[1], David Bulmer[2,3], Nicolas Cenac[1*]

Affiliations:

[1] INSERM, UMR1220, IRSD, Université de Toulouse, INRA, ENVT, UPS, Toulouse, France
[2] Department of Pharmacology, University of Cambridge, Tennis Court Road, Cambridge CB1 2PD, UK
[3] National Centre for Bowel Research and Surgical Innovation, Blizard Institute, Barts and the London School of Medicine and Dentistry, Queen Mary University of London, London E1 2AJ, UK
[4] INSERM UMR1048, Lipidomic Core Facility, Metatoul Platform, Université de Toulouse, Toulouse, France
[5] Department of Medical and Surgical Sciences, University of Bologna, Bologna, Italy
[6] Aix-Marseille-Université, CNRS, Institut de Biologie du Développement de Marseille, UMR 7288, Marseille, France.
[7] Neuro-Gastroenterology and Nutrition Team, UMR 1331, INRA Toxalim, INP-EI-Purpan, Université de Toulouse, Toulouse, France
[8] Institute of Neuroscience and Psychology, University of Glasgow, Glasgow, United Kingdom

† Joint as first author

Current address: Snyder Institute for Chronic Diseases, Cumming School of Medicine, University of Calgary, 3330 Hospital Drive N.W., Calgary, Alberta, Canada, T2N 4N1

*** Corresponding author:**
Nicolas Cenac
INSERM IRSD U1220
CHU Purpan
Place du docteur Baylac ; CS 60039
31024 Toulouse cedex 3 ; France
+33531 547 917
nicolas.cenac@inserm.fr

One Sentence Summary: The bioactive lipid 5-oxoETE is specifically increased in constipation predominant irritable bowel syndrome and mediates nociception through a novel MAS-related G protein coupled receptor D (Mrgprd) pathway.

Abstract

Irritable bowel syndrome (IBS) is a common gastrointestinal disorder characterized by chronic abdominal pain concurrent with altered bowel habit. Polyunsaturated fatty acid (PUFA) metabolites such as prostaglandin E2 (PGE_2) are elevated in IBS and implicated in visceral hypersensitivity. The aim of this study was to quantify PUFA metabolites in IBS patients and evaluate their role in pain. Quantification of PUFA metabolites by mass spectrometry in colonic biopsies showed an increase in 5-oxo-eicosatetraenoic acid (5-oxoETE) only in biopsies taken from IBS with predominant constipation (IBS-C) patients. Local 5-oxoETE administration induced somatic and visceral hypersensitivity with no tissue inflammation. 5-oxoETE directly acts on both human and mouse sensory neurons as shown by lumbar splanchnic nerve recordings and Ca^{2+}-imaging of dorsal root ganglia (DRG) neurons. 5-oxoETE selectively stimulated isolectin B4 (IB4)-positive DRG neurons through a PLC and pertussis toxin-dependent mechanism, suggesting a G-protein coupled receptor-mediated effect. The MAS-related G protein coupled receptor D (Mrgprd) was found in mouse colonic DRG afferents and was identified as the target receptor for 5-oxoETE. In conclusion, 5-oxoETE, a potential biomarker of IBS-C, activates Mrgprd in nociceptors and induces somatic and visceral hyperalgesia without inflammation. Thus, 5-oxoETE may play a pivotal role in abdominal pain associated with IBS-C.

Introduction

IBS is a functional bowel disorder in which recurrent abdominal pain is associated with a change in bowel habit, typically constipation (IBS-C), diarrhea (IBS-D), or a mixed (constipation and diarrhea) bowel habit (IBS-M) (1). IBS is a common disorder in Western populations affecting around 11% of the global population (*2*), with a higher prevalence in women than men (1). Although the aetiology of IBS remains unclear, low-grade inflammation has been widely described in this disorder, with several fundamental studies implicating pro-inflammatory molecules in the pathophysiology of IBS symptoms (*3*). We have previously shown that the levels of several PUFA metabolites, also defined as bioactive lipids, are significantly altered in biopsy samples from IBS patients compared to controls (*4*). This is in agreement with previous studies focused on the prostanoid subtype of PUFA metabolites (*5-7*).

The functional relationship between PUFAs and pain has been the subject of many studies (*8*). Both basic and clinical studies have revealed that a dietary intake of n-3 series PUFAs results in a reduction in pain associated with rheumatoid arthritis (*9, 10*), dysmenorrhea (*11*), inflammatory bowel disease (*12*), and neuropathy (*13*), while n-6 series PUFAs are high in patients with chronic pain including IBS patients (*4, 14, 15*). N-3 PUFA metabolites such as resolvins (Rv) are analgesic in multiple pain models, an effect attributed to inhibition of certain transient receptor potential (TRP) channels (*16*). For example, RvE1 has been shown to specifically inhibit TRPV1 signaling (*17*), while RvD1 attenuates the function of TRPA1 and TRPV4 (*18*) and RvD2 inhibits TRPV1 and TRPA1 activity (*19*). These effects have been observed with other types of n-3 PUFAs such as maresin 1 (Mar1), which also has inhibitory effects on TRPV1 channel function (*20*) and reduces pain. The quantification of Rvs in knee synovia of patients suffering from inflammatory arthritis suggests that synthesis of specialized pro-resolving mediators (SPM) at the site of inflammation may be a mechanism of endogenous pain relief in humans. In contrast, n-6 PUFA metabolites have been shown to be pro-nociceptive

by stimulating nerve fibers via the activation of immune cells (*21*, *22*). Nonetheless, several n-6 PUFA metabolites such as thromboxane A_2 (TXA_2), PGE_2, leukotriene B4 (LtB4) and PGD_2, can directly stimulate sensory nerve fibers (*23*-*26*). Although, some n-6 PUFA metabolites, such as lipoxins, can inhibit pain (*27*). Consistent with the role of TRP channels in the transduction of noxious stimuli, we have previously shown a robust correlation between PUFA metabolites and TRP channel activation, particularly for the TRPV4 agonist 5,6-epoxyeicosatrienoic acid (5,6-EET) and pain intensity in IBS-D patients (*4*). Interestingly, PUFA metabolites from colonic biopsies of IBS-C patients induced Ca^{2+} influx in sensory neurons independently of TRPV4, suggesting that the PUFA metabolites produced in IBS-C and IBS-D are distinct (*4*). Thus, the aim of this study was to identify algogenic PUFA metabolites specifically produced in IBS-C patients and decipher the mechanism by which they may activate sensory nerves. Herein, we show that 5-oxoETE, an n-6 PUFA subtype selectively increased in colonic tissues from IBS-C patients, induces hypersensitivity through Mrgprd activation.

Results

5-oxoETE is increased in colonic biopsies from IBS-C patients

PUFA metabolites were quantified in colonic biopsies from IBS patients and healthy controls (HC) using liquid chromatography/tandem mass spectrometry (LC-MS/MS). Hierarchical clustering of PUFA metabolite amounts quantified in biopsies (pg/mg of protein) was used to reveal the main differences between HC, IBS-M, IBS-C and IBS-D patients (Fig.1A). PUFA metabolites formed 5 different clusters. The first cluster contained products of arachidonic acid metabolism (PGE_2, TXB_2, 5,6-EET and 14,15-EET), eicosapentaenoic acid metabolism (18-HEPE, LtB5 and PGE_3) and PDx. This first cluster of metabolites was higher in biopsies from IBS-D patients (Fig.1A). Of note, TxB_2, PGE_2 and 5,6-EET were only increased in biopsies of IBS-D patients (Fig. S1). By contrast, TxB_2 was decreased in biopsies from IBS-C patients (Fig. S1). The second cluster discriminated only 5-oxoETE, which was significantly elevated in biopsies from IBS-C patients (Fig.1A and 1B). The concentration of 7-MaR1 and $15dPGJ_2$, delineated a third cluster, which although presenting a trend towards increasing levels, did not reach statistical significance in biopsies from any group of IBS patients (Fig. S2). The fourth cluster, grouping the majority of lipoxygenase-derived metabolites, was decreased in biopsies from all subtypes of IBS patients (Fig.1A). 15-, 5-, 12-HETE and 14-, 17-HDoHE were significantly decreased in all IBS patients (Fig. S2). In addition, 12-HETE was significantly decreased in biopsies from IBS-C patients (Fig. S1). The metabolites included in the fifth cluster were reduced only in biopsies from IBS-C and IBS–D (Fig.1A). RvD1 and RvD2 were not detectable in any colonic biopsies.

Thus, amongst all PUFA metabolites quantified in colonic biopsies from IBS patients, 5-oxoETE was the only one to be significantly upregulated in IBS-C patients compared to the other IBS subtypes (Fig.1B) and thus warranted further investigation.

Local administration of 5-oxoETE induces somatic and visceral hyperalgesia without inflammation

As PUFA metabolites can stimulate the immune system and/or directly stimulate nerves, we first assessed the effect of 5-oxoETE on pain and inflammation processes *in vivo.* In a first set of experiments, 5-oxoETE was subcutaneously injected into the paw of mice and the paw-withdrawal threshold to mechanical stimuli was estimated using calibrated von Frey filaments. The time course of mechanical hypersensitivity of the mice receiving 5-oxoETE was compared with that of mice injected with vehicle (HBSS). Basal mechanical sensitivity, measured in the paw before injection, was identical in both groups of mice (Fig.2A). Injection of 5-oxoETE into hind paws resulted in a decrease of the paw-withdrawal threshold (Fig.2A) and was observed from 15 min up to 2 hours after 5-oxoETE injection, with a peak reduction at 30 min. The mechanical pain threshold was decreased in a dose-dependent manner 30 min after 5-oxoETE administration with an EC_{50} of 0.6 µM (Fig.2B). In addition, paw edema formation and histological analysis were investigated to verify whether injection of 5-oxoETE induced an inflammatory process or not. Injection of 5-oxoETE into the hind paw did not induce paw edema (Fig. S3). Moreover, histological analysis of paw tissue did not reveal any sign of inflammation. Likewise, neither tissue disruption nor cellular infiltration was observed even 6 hours after injection of 100 µM of 5-oxoETE (Fig.2C). Thus, at the somatic level, 5-oxoETE increased paw sensitivity to mechanical stimulation without inducing quantifiable inflammatory reaction.

Intracolonic administration of 5-oxoETE resulted in an increased intensity of abdominal contractions in response to colorectal distension (Fig.2D). Moreover, the increased intensity of abdominal contractions was observed in response to both innocuous (allodynia) and noxious (hyperalgesia) stimuli 30 min after 5-oxoETE treatment (Fig.2D). Intracolonic treatment with vehicle (40% ethanol) did not alter abdominal contraction response (Fig.2D). As observed

following subcutaneous hind paw injection, intracolonic administration of 5-oxoETE did not induce inflammation of the colon. Colonic inflammation was assessed by macroscopic scoring and myeloperoxidase activity, which were not increased by 5-oxoETE administration when compared to vehicle (Fig. S3). Moreover, histological analysis did not reveal intestinal wall thickening, leukocyte infiltration into the *lamina propria*, presence of ulceration or goblet cell depletion (Fig.2E).

Thus, *in vivo* local administration of 5-oxoETE induces visceral hyperalgesia in the absence of inflammation, thus suggesting a direct effect on nociceptors.

5-oxoETE stimulates visceral and somatic nociceptors: translation to human DRG

To confirm a direct effect of 5-oxoETE on sensory nerves, we examined its effects upon nerve discharge in mouse colonic nociceptors. Application of 100 µM of 5-oxoETE induced an axonal discharge in 38% of lumbar splanchnic (colonic) nerve fibers assessed (Fig.3). In a second set of experiments, we determined the effect of 5-oxoETE on Ca^{2+} mobilization in primary cultures of neurons from mouse DRG. In preliminary experiments performed with a working solution containing Ca^{2+} and Mg^{2+}, we observed a transient increase in $[Ca^{2+}]_i$ (data not shown). To determine if this transient increase was the consequence of intracellular Ca^{2+} release or influx of external Ca^{2+}, experiments were performed without Ca^{2+} and Mg^{2+} in the extracellular solution. Even without Ca^{2+} in the extracellular compartment, 5-oxoETE evoked a transient increase in $[Ca^{2+}]_i$ that was maximal after 10–20 seconds and declined to baseline afterwards (Fig.4A). The mobilization of intracellular Ca^{2+} by 5-oxoETE treatment was concentration-dependent (Fig.4B). Similarly, 5-oxoETE also induced an increase in $[Ca^{2}{}_{+]i}$ and the percentage of responding neurons in a concentration-dependent manner in human primary sensory neurons (Fig.4C).

Thus, our data indicate that 5-oxoETE directly activates colonic DRG neurons from mice, as well as human sensory neurons, inducing an increase in $[Ca^{2+}]_i$ (Fig.4) and nociceptor firing (Fig.3).

As 5-oxoETE induces somatic pain without inflammation *in vivo*, we hypothesised that 5-oxoETE predominantly activates $IB4^+$ sensory neurons, which do not release neuropeptides involved in neurogenic inflammation. To assess our hypothesis, mouse sensory neurons were labelled with isolectin B4 and treated with 10 µM 5-oxoETE without Ca^{2+} in the extracellular medium. 5-oxoETE induced an increase in $[Ca^{2+}]_i$ in more than 50% of IB4-positive neurons, but not in IB4-negative neurons (Fig.4D). To decipher the intracellular pathway responsible for the intracellular Ca^{2+} mobilization by 5-oxoETE, sensory neurons were pretreated with pertussis toxin (PTX, a G_i, G protein inhibitor) or the PLC inhibitor U73122. In neurons pretreated with the pertussis toxin (PTX; 250 ng/ml), the increase in $[Ca^{2+}]_i$ induced by 5-oxoETE was significantly decreased (Fig.4E). Pre-treatment of sensory neurons with U73122 (10µM) also inhibited the increase in $[Ca^{2+}]_i$ induced by 5-oxoETE (Fig.4E).

Thus, 5-oxoETE directly stimulates IB4-positive sensory neurons via a $G\alpha_{i/o}/G\alpha_q$-coupled, G-protein-coupled receptor.

5-oxoETE activates sensory neurons and induces visceral hypersensitivity via Mrgprd

Due to 5-oxoETE specifically activating $IB4^+$ sensory neurons via $G\alpha_i$-protein-mediated signalling pathways, we focused our attention on the MAS-related G protein receptor D (Mrgprd), which is $G\alpha_{i/o}/G\alpha_q$ coupled. The expression and function of Mrgprd in polymodal nociceptors innervating the skin is well established (*28*), however for visceral tissues this remains less clear. In order to comprehensively assess this, we retrogradely labelled sensory afferents from the colon using microinjection of Fast Blue (FB) in wild-type mice and $Mrgprd^{EGFP}$-tagged mice. Single-cell qRT-PCR was performed on FB-expressing cells from

the dorsal root ganglia from wild-type mice. *Mrgprd* mRNA was detected at some level in 40% (18/45) of FB-labelled sensory neurons projecting to the colon via the splanchnic nerve originating from thoracolumbar (T10-L1) DRG (Fig.5A). *Trpv1* mRNA was observed in 82% (37/45) of cells, with 41% (15/37) of *Trpv1*-positive neurons also expressing *Mrgprd* mRNA (Fig.5A). Immunohistochemistry was performed on the T13 DRG from the *Mrgprd*^{EGFP}-tagged mice to determine the incidence of GFP-expression and the peptidergic marker calcitonin gene related peptide (CGRP) in FB-labelled cells, revealing two distinct non-overlapping populations (Fig.5B). In agreement with previous studies, those sensory neurons labelled from the colon with the retrograde tracer Fast-Blue were predominantly CGRP-positive (~70%). By contrast, GFP immunoreactivity was observed in a restricted subset of colonic sensory neurons, accounting for only 7% of FB-labelled cells (Fig. 5B and Table 2). Of the 274 FB+ cells assessed, only cell one co-expressed both Mrgprd and CGRP. Those neurons projecting to the viscera represent ~10% of the total population of T10-L1 DRG neurons. Thus, only a very small population (between less than 1% and 4%) of T10-L1 DRG neurons are likely to be both colon projecting and Mrgprd-positive.

In experiments using an antibody against Mrgprd, we observed, infrequent yet reproducible, co-localisation of Mrgprd with PGP9.5 in the colon of 6 wild-type mice out of 10 assessed (Fig.S4). Importantly, Mrgprd immunoreactivity was not observed in the colon of Mrgprd-deficient mice (Fig.S4). The expression of Mrgprd was also assessed in human sensory neurons. As shown in Fig.5C, Mrgprd immunoreactivity was present in 22% of human T11 DRG neurons, which also co-expressed the pan-neuronal marker PGP9.5. In a culture of human sensory neurons, 20% of PGP9.5-positive neurons possessed Mrgprd immunoreactivity (Fig.5D).

To demonstrate the role of Mrgprd in 5-oxoETE-induced neuronal firing, its expression was silenced by transducing primary cultures of mouse sensory DRG neurons with a

recombinant lentivirus expressing a shRNA directed against *Mrgprd* and the gene reporter red fluorescent protein (RFP). As a control, neurons were transduced with a lentivirus expressing a scrambled shRNA. As expected, the percentage of neurons responding to 5-oxoETE was significantly reduced in sensory neurons expressing shRNA against *Mrgprd* compared to those neurons expressing the scrambled shRNA (Fig.6A). Accordingly, application of 5-oxoETE on sensory neurons from Mrgprd-deficient mice had no greater effect than HBSS alone (Fig.6B). In contrast, treatment of Mrgprd-deficient sensory neurons with a mix of GPCR agonists (bradykinin, serotonin and histamine, 10 µM each), used as a positive control, induced an increase in $[Ca^{2+}]_i$ (Fig.6B). Reciprocally, 5-oxoETE induced a concentration-dependent increase in $[Ca^{2+}]_i$ only in *Mrgprd*-transfected CHO cells (Fig.6C). In a last set of experiments, the sensitivity to colorectal distension was assessed in Mrgprd-deficient mice 30 min after intracolonic administration of 5-oxoETE (10 µM). In contrasting to wild-type mice, 5-oxoETE did not induce hypersensitivity in response to colorectal distension in Mrgprd-deficient mice (Fig.6D).

Discussion

Our results show that: 1) Concentrations of the PUFA metabolite 5-oxoETE are significantly increased in biopsies from patients with IBS-C compared to other IBS subtypes and healthy controls; 2) 5-oxoETE induces somatic, as well as visceral hyperalgesia, without promoting inflammation; 3) 5-oxoETE activates both mouse and human sensory neurons; 4) In mouse, 5-oxoETE signals through Mrgprd. Taken together, these data clearly highlight a role for 5-oxoETE and Mrgprd-expressing IB4-positive sensory neurons in visceral hypersensitivity in IBS-C patients.

Eicosanoids and docosanoids are the most important lipids implicated in inflammatory processes; they derive from the oxidation of twenty and twenty-two carbon PUFA, respectively (*29*). Several PUFA metabolites increased in the intestinal mucosa from patients with inflammatory bowel diseases such as TXA_2, PGE_2, LTB_4 or PGD_2 induce visceral afferent fiber activation (*23-26*). Here, we show that PGE_2, 5,6-EET and TXB_2 are significantly increased in the intestinal mucosa of IBS-D patients while no alteration of PUFA metabolism was observed in IBS-M. Interestingly, if lipid extracts from controls and all IBS patients are compared, a significant decrease in 14-HDoHE and 17-HDoHE which are precursors of specialized pro-resolving mediators (SPM) (*30*), is observed. As SPM possess an analgesic effect (*31*), the pain associated with IBS could be also the consequence of a decrease in SPM leading to sensory neuron activation. A complete characterization of the different SPM produced by EPA, DHA or DPA metabolism will be of interest for the characterization of bioactive lipids potentially linked with pain in IBS patients.

We show that the concentration of 5-oxoETE only increases in colonic biopsies of IBS-C patients highlighting its potential relevance as a new marker of the disease. 5-oxoETE, which derives from arachidonic acid (AA) metabolism, is produced by a variety of inflammatory cells. Additionally, it can also be synthesized from 5-HETE by stromal cells, possibly by transcellular

biosynthesis (*32*). 5-oxoETE is formed by the oxidation of 5-HETE by 5-hydroxyeicosanoid dehydrogenase (5-HEDH) (*33*), a microsomal enzyme that is highly selective for 5S-HETE and requires $NADP^+$ as a cofactor (*34*). 5-HEDH is found in neutrophils as well as in a variety of other inflammatory and stromal cells, including monocytes (*35*), dendritic cells (*36*) and intestinal epithelial cells (*37*). 5-oxoETE has been widely shown to be a potent chemoattractant for human and rat eosinophils and to indirectly promote the survival of these cells (*38*). Nevertheless, no cellular infiltration was observed either in the paw or intestinal mucosa of mice administered with 5-oxoETE. This discrepancy may be due to the rapid metabolism of 5-oxoETE *in vivo* (*32*) or the absence of other molecules such as interleukin-5 acting in synergy to attract inflammatory cells during inflammatory processes or allergies (*39*). In our experiments, the injection of 5-oxoETE alone, without cofactors, could thus explain the absence of infiltration by polymorphonuclear cells. Formation of 5-oxoETE needs $NADP^+$ (*40*). Accordingly, oxidative stress associated with IBS-C (*41*) may improve the conversion rate of NADPH into $NADP^+$ in epithelial cells, thereby resulting in the synthesis of larger amounts of 5-oxoETE.

In a previous study, we reported that PUFA metabolites extracted from biopsies of IBS-C and IBS-D patients triggered an increase in $[Ca^{2+}]_i$ in primary sensory neurons, while those of IBS-M had no effect (*4*). We further identified the PUFA metabolite 5,6-EET as a TRPV4 agonist with algogenic activity, specifically associated with IBS-D sub-group (*4*). By contrast, no PUFA metabolite with TRP agonist activity was found to be increased in IBS-C patient biopsies (*4*). Since only 5-oxoETE is increased in biopsies of IBS-C patients, we hypothesized that this PUFA metabolite may be responsible for the activation of sensory neurons and hypersensitivity-associated with IBS-C. As previously reported in humans, 5-oxoETE may interact with OXE receptor. However, there is no homologous OXE receptor in rodents (*40*). Since the observed 5-oxoETE-induced increase in $[Ca^{2+}]_i$ in mouse sensory neurons was

inhibited by both PLC inhibitor and pertussis toxin (PTX), we hypothesized that 5-oxoETE binds to $G\alpha_{i/o}/G\alpha_q$ protein-coupled receptors. Given that 5-oxoETE acts selectively on $IB4^+$ sensory neurons, the targeted receptor should be specifically expressed on this neuronal subclass. Accordingly, we investigated the role of MAS-related G protein coupled receptor D (Mrgprd), a receptor specifically expressed on $IB4^+$ sensory neurons, which may be coupled to $G\alpha_q$ protein and to PTX–sensitive $G\alpha_{i/o}$ proteins (*42*), previously reported as a key player in mechanical hypersensitivity (*43-45*).

Stimulation of Mrgprd positive neurons with β-alanine, the prototypical agonist of Mrgprd, increased $[Ca^{2+}]_i$, as observed here after 5-oxoETE treatment (*46*). Moreover, in a FLIPR (Fluorescent Imaging Plate Reader) assay developed for the simultaneous identification of Mrgprd agonists and antagonists, a PLC inhibitor completely blocked the FLIPR response to β-alanine while PTX treatment resulted in 50% reduction in $[Ca^{2+}]$ (*47*). Again, similar results were obtained here by using PTX or PLC inhibitor to inhibit 5-oxoETE-induced activation of primary mouse sensory neurons. Using tissue from adult *Mrgprd*^{EGFP} mice stained with antibodies to GFP, a previous study showed that Mrgprd is expressed in non-peptidergic neurons that innervate the epidermis, but failed to observe Mrgprd-positive fibres in any other visceral organs including both the small and large intestine (*28*). By contrast, numerous studies using different retrograde tracers have identified a minor population (20-26%) of $IB4^+$ sensory neurons that innervate the colon (*48-50*). Indeed, a recent study also identified *Mrgprd* mRNA in colonic sensory neurons by single cell RNA-sequencing (*51*). In order to confirm the presence of both *Mrgprd* mRNA and Mrgprd protein expression in colonic sensory neurons in the present study, we applied a similar retrograde neurotracing approach using single cell RT-qPCR and anti-GFP immunostaining in *Mrgprd*^{EGFP} mice. We observed *Mrgprd* mRNA and Mrgprd protein expression in sensory DRG neurons projecting to the colon at similar frequency to that observed in previous studies (*51*), thereby not only confirming the presence of a Mrgprd-

positive colonic neuronal subtype, but also reinforcing Mrgprd as a potential target of 5-oxoETE. The activity of 5-oxoETE towards Mrgprd was attested to by its ability to induce an increase in $[Ca^{2+}]_i$ in IB4-positive sensory neurons, but not in lentivirus-mediated *Mrgprd* knocked-down or Mrgprd-deficient mouse neurons. Conversely, while Ca^{2+} transients were triggered in CHO cells transfected with a *Mrgprd*-expression plasmid, CHO cells transfected with a control plasmid were not responsive to 5-oxoETE.

Activation of Mrgprd inhibits a fraction of the total M-current, carried primarily by the KCNQ2/3 K^+ channel, contributing to an increase in excitability of DRG neurons (*52*). Thus, Mrgprd activation by 5-oxoETE might promote the excitability of primary nociceptive afferents by KCNQ inhibition. Several groups have demonstrated that retigabine, a KCNQ2–5 opener, is effective in reducing neuropathic (*53*) and inflammatory pain (*54*). At the visceral level, retigabine reduces capsaicin-induced visceral pain and can inhibit noxious chemosensitivity in human tissue indicating that KCNQ channels play an inhibitory role in the transmission of visceral nociception (*55, 56*). Given that human sensory DRG neurons express Mrgprd and are activated by 5-oxoETE, we may assume that 5-oxoETE modulates KCNQ channels via Mrgprd activation leading to neuronal activation contributing to pain symptoms associated with IBS-C. Nevertheless, as OXER1 is expressed in human tissue, we cannot exclude an activation of this receptor by 5-oxoETE in human tissue. Taken together, our results strengthen previous findings from our laboratory showing a pivotal role of PUFA metabolites in visceral pain associated with IBS (*4*). Specifically, our study identifies 5-oxoETE with pro-nociceptive activity, as a hallmark of IBS-C subtype.

Materials and methods

Chemicals

6-keto-prostaglandin F1α (6kPGF$_{1\alpha}$), thromboxane B2 (TXB$_2$), prostaglandin E2 (PGE$_2$), prostaglandin A1 (PGA$_1$), 8-iso prostaglandin A2 (8-iso PGA$_2$), prostaglandin E3 (PGE$_3$), 15-deoxy-$\Delta^{12,14}$-prostaglandin J2 (15d-PGJ$_2$), lipoxin A4 (LxA4), lipoxin B4 (LxB4), lipoxin A4 deuterated (LxA4-d5), resolvin D1 (RvD1), resolvin D2 (RvD2), 7-maresin (7-MaR1), leukotriene B4 (LTB4), leukotriene B5 (LTB5), leukotriene B4 deuterated (LTB4-d4), 10(S),17(S)-protectin (PDx), 18-hydroxyeicosapentaenoic acid (18-HEPE), dihydroxy-eicosatetraenoic acid (5,6-DiHETE), 15-hydroxyeicosatetraenoic acid (15-HETE) and 12-HETE, 8-HETE, 5-HETE, 5-HETE-d8, 17-hydroxy-docosahexaenoic acid (17-HDoHE) and 14-HDoHE, 14,15-epoxyeicosatrienoic acid (14,15-EET) and 11,12-EET, 8,9-EET, 5,6- EET, 5-oxoeicosatetraenoic acid (5-oxoETE) were purchased from Cayman Chemicals (Ann Arbor, MI, USA).

Patients

Patients (Table 1) were recruited from outpatient clinics of the Department of Medical and Surgical Sciences of the University of Bologna (Italy), and were included according to Rome III criteria for IBS. Healthy controls (HC) were asymptomatic subjects undergoing colonoscopy for colorectal cancer screening. In this group, we excluded subjects based on the presence of the following symptoms in the last 12 months: abdominal discomfort or pain, bloating, and bowel habit changes. Exclusion criteria for both IBS and HC included major abdominal surgery, any organic syndrome, celiac disease (excluded by detection of anti-transglutaminase and anti-endomysial antibodies), asthma, food allergy, or other allergic disorders. None of these patients or HC were taking nonsteroidal anti-inflammatory drugs or any other anti-inflammatory drugs (including steroids, antihistamines, and mast cell stabilizers). Patients and HC gave written

informed consent. The study protocol was approved by the local Ethic Committee (64/2004/O/Sper and EM14/2006/O) and conducted in accordance with the Declaration of Helsinki. Patients underwent colonoscopy and, in all cases, 6 mucosal biopsies were obtained from the proximal descending colon. One biopsy was sent to the pathology department for exclusion of microscopic colitis or other microscopic tissue abnormalities and 4 were used in other studies. One biopsy was snap-frozen in liquid nitrogen for lipid extraction and PUFA quantification for the purpose of our study.

Lipid extraction

Biopsies were crushed with a FastPrep®-24 Instrument (MP Biomedicals, Illkirch, France) in 500 µL of Hank's balanced salt solution (HBSS, Invitrogen, Villebon sur Yvette, France) and 5 µL of internal standard mixture (LxA4-d5, LTB4-d4 and 5-HETE-d8 at 400 ng/mL in MeOH). After 2 crush cycles (6.5 m/s, 30 s), 10 µL were withdrawn for protein quantification and 300 µL of cold methanol were added. Samples were centrifuged at 1000 g for 15 min at 4 °C. Supernatants were collected, completed to 2 mL in H_2O and submitted to solid-phase extraction using HRX-50 mg 96-well (Macherey Nagel, Hoerd, France). Briefly, after plate conditioning, the sample was loaded at flow rate of 0.1 mL/min. After complete loading, the plate was washed with H_2O/MeOH (90:10, 2 mL) and lipid mediators were eluted with MeOH (2 mL). Solvent was evaporated under nitrogen and samples were dissolved with MeOH and stored at -80 °C for liquid chromatography/tandem mass spectrometry measurements.

Liquid chromatography/tandem mass spectrometry (LC-MS/MS) measurements

6kPGF1α, TXB_2, PGE_2, PGA_1, 8-isoPGA_2, PGE_3, 15d-PGJ_2, LxA4, LxB4, RvD1, RvD2, 7-MaR1, LTB4, LTB5, PDx, 18-HEPE, 5,6-DiHETE, 15-HETE, 12-HETE, 8-HETE, 5-HETE, 17-HDoHE, 14-HDoHE, 14,15-EET, 11,12-EET, 8,9-EET, 5,6-EET and 5-oxo-ETE were

quantified in human biopsies (*57*). To simultaneously separate 28 lipids of interest and 3 deuterated internal standards, LC-MS/MS analysis was performed on ultra high performance liquid chromatography system (UHPLC, Agilent LC1290 Infinity) coupled to Agilent 6460 triple quadrupole MS (Agilent Technologies) equipped with electro-spray ionization operating in negative mode. Reverse-phase UHPLC was performed using ZorBAX SB-C18 column (Agilent Technologies) with a gradient elution. The mobile phases consisted of water, acetonitrile (ACN) and formic acid (FA) (75:25:0.1; v/v/v) (A) and ACN, FA (100:0.1, v/v) (B). The linear gradient was as follows: 0% B at 0 min, 85% B at 8.5 min, 100% B at 9.5 min, 100% B at 10.5 min and 0% B at 12 min. The flow rate was 0.35 mL/min. The autosampler was set at 5 °C and the injection volume was 5 µL. Data were acquired in Multiple Reaction Monitoring (MRM) mode with optimized conditions. Peak detection, integration and quantitative analysis were done using Mass Hunter Quantitative analysis software (Agilent Technologies). For each standard, calibration curves were built using 10 solutions at concentrations ranging from 0.95 ng/mL to 500 ng/mL. A linear regression with a weight factor of 1/X was applied for each compound. The limit of detection (LOD) and the limit of quantification (LOQ) were determined for the 28 compounds using signal to noise ratio (S/N). The LOD corresponded to the lowest concentration leading to a signal to noise over 3 and LOQ corresponded to the lowest concentration leading to a signal to noise over 10. All values under the LOQ were not considered. Blank samples were evaluated, and their injection showed no interference (no peak detected), during the analysis. Hierarchical clustering and heat-map were obtained with R (www.r-project.org). PUFA metabolite amounts were transformed to z-scores and clustered based on 1-Pearson correlation coefficient as distance and the Ward algorithm as agglomeration criterion.

Animals

C57BL/6 male mice (3 weeks-old) were purchased from Janvier (Le Genest Saint Isle, France). Mrgprd$^{cre/+}$ mice were a generous gift from Dr D. Anderson at Caltech Pasadena. These mice were previously generated by Rau et al 2009 (*44*) and were in an almost pure C57/Bl6J background when we received them at IBDM (Institut de Biologie du Développement de Marseille) mouse facility. There, the mice were kept as heterozygous and were backcrossed to C57/Bl6J for another 8 generations. Mrgprd deficient mice used in this study were obtained by intercrossing Mrgprd$^{cre/+}$ heterozygous mice. Animals were maintained in ventilated cages (4 mice per cage) in a specific pathogen free room at 20–24 °C and relative humidity (40%–70%) with a 12 hours light/dark cycle and given free access to food and water. Animal Care and ethic Committee of US006/CREFE (CEEA-122) approved the whole study protocol (permit No. MP/01/64/09/12). *Mrgprd*^{EGFP}-tagged mice (B6;129SP2-*Mrgprd*$^{tm4.1(COP4)Mjz}$/Mmnc; MMRRC, North Carolina, USA) were raised and maintained at the University of Glasgow, and have been characterised previously (*58*). Experiments conducted at the University of Glasgow were approved by the University's Ethical Review Process Applications Panel, and were performed in accordance with the European Community directive 86/609/EC and the United Kingdom Animals (Scientific Procedures) Act 1986.

Measurement of somatic nociception

Paw-withdrawal thresholds were measured using calibrated von Frey filaments with forces ranging from 0.04 to 2 g (Stoelting, Wood Dale, IL, USA), which were applied onto the plantar surface of mice. Ascending series of von Frey filaments were applied with each monofilament being tested 5 times for approximately 1 second. Threshold to mechanical stimuli was calculated as the force value of the von Frey filament triggering 3 paw withdrawals over 5 applications (*59*). Responses to mechanical stimuli were recorded before and 15 min, 30 min,

1 hour, 2 hours and 6 hours after an intraplantar injection of 0.1, 1, 10 or 100 µM of 5-oxoETE or its vehicle (HBSS). In a second set of experiments, paw edema was measured using digital calipers (resolution 0.01; Mitutoyo, Aurora, IL, USA) at 1, 2, 3 and 4 hours after intraplantar injection of 100 µM of 5-oxoETE. At the end of the experiment, paws were collected for histological analysis by hematoxylin and eosin staining (H&E).

Colorectal distension (CRD) and electromyography recordings

Mice were administered either 100 µL of 5-oxoETE (10 µM) or its vehicle (40% ethanol) intracolonically. We performed a session of CRD and recorded visceromotor responses (VMR) from implanted electrodes before and 30 min after treatment as previously described (*60*). Data are presented as the difference between the VMR induced by the distension performed before and after intracolonic treatments. After distension, mouse colons were harvested to perform histological analysis (H&E) and myeloperoxidase activity assay.

Lumbar splanchnic nerve recording

The distal colon with associated lumbar splanchnic nerves was removed from male C57BL/6 mice (12 weeks). The colon was then opened along the anti-mesenteric border and pinned flat mucosal side up. The tissue was perfused (7 mL/min; 32-34 ℃) with carbogenated Krebs buffer (in mM: 124 NaCl; 4.8 KCl; 1.3 NaH2PO4; 2.4 CaCl2; 1.2 MgSO4.7H2O; 11.1 glucose; 25 NaHCO3) and supplemented with 10 µM nifedipine and 10 µM atropine to block smooth muscle contraction, and 3 µM indomethacin to inhibit endogenous prostanoid production. Single unit activity was discriminated using wave form analysis software (Spike 2 Cambridge Electronic Design) from fibers teased from the lumbar splanchnic nerve (rostral to the inferior mesenteric ganglia), recorded using borosilicate glass suction electrodes. Signals were amplified, band pass filtered (gain 5K; 100-1300 Hz; Neurology, Digitiser Ltd, UK), digitally

filtered for 50Hz noise (Humbug, Quest Scientific, Canada), digitalised at 20 kHz (micro1401; Cambridge Electronic Design, UK) and displayed on a computer using Spike 2 software. Individual receptive fields of afferent nerve fibers were identified by systematically probing the tissue with a 1 g von Frey filament. Receptive fields that responded to probing and not to stretch were identified as serosal units (*61*). Once a serosal unit was identified a metal ring was placed over the receptive field and the baseline activity was observed for 3 min. The Krebs solution within the ring was then removed and replaced by 100 µM 5-oxoETE pre-warmed to bath temperature. Following a 7 min challenge period the 5-oxoETE and ring were removed.

Immunofluorescence in mouse colon

The descending colons of 10 wild-type and 10 Mrgprd deficient mouse were cryoprotected in OCT compound, sectioned at a thickness of 10 µm (one every 0.1 cm, 20 per mouse) on a cryostat (Leica CM1950, Nanterre, France), and mounted on Superfrost slides (Thermo Fisher Scientific, Villebonne-sur-Yvette, France). Slides were washed in phosphate buffered saline (PBS), 0.5% Triton X-100, and 1% bovine serum albumin (BSA) solution (Sigma, Saint-Quentin Fallavier, France) and incubated overnight at 4°C with the primary antibodies anti–Mrgprd (1:500, AMR-061, Alomone labs, Clinisciences, Nanterre, France) and anti-PGP9.5 (1:500, AB86808, Abcam, Coger SAS, Paris, France). After washing, slides were incubated with the appropriate secondary antibody conjugated with Alexa Fluor® 488 or Alexa Fluor® 555 (Thermo Fisher Scientific), washed, and mounted with ProLong Gold reagent containing DAPI (Molecular Probes). Images were acquired using Zeiss LSM-710 confocal microscopes (Carl Zeiss MicroImaging, Jena, Germany) with 20X objective in the inverted configuration.

Single-cell qRT-PCR of retrogradely labelled mouse sensory neurons

Dorsal root ganglia neurons projecting to the colon were selectively labelled, individually harvested by pulled glass pipette. After RNA extraction, single-cell RT-qPCR for the presence of *Mrgprd* mRNA transcripts was performed as previously described (*62*). In brief, adult mice were subjected to laparotomy under anesthesia and 6-8 injections of Fast Blue (~ 0.2 µL, 2 % in saline; Polysciences GmbH) were made into the wall of the distal colon. Five days post-surgery, thoracolumbar (TL; T10-L1) DRG were collected and enzymatically dissociated (*62*). Individual cells were isolated by pulled glass pipette and collected into a preamplification mastermix containing 0.1 µL SUPERase-in (Ambion, TX, USA), 0.2 µL Superscript III Reverse Transcriptase/Platinum Taq mix (Invitrogen), 5 µL CellDirect 2x reaction buffer (Invitrogen), 2.5 µL 0.2x primer/probe mix and 1.2 µL TE buffer (Applichem, GmbH) before thermal cycling (50 °C for 30 min, 95 °C for 2 min, then 21 cycles of (95 °C for 15 seconds, 60 °C for 4 min)). TaqMan qPCR assays for *Mrgprd* (TaqMan Assay ID: Mm01701850_s1) and *Trpv1* (Mm01246300_m1) were performed on diluted cDNA products (1:5 in TE buffer) using the following cycling protocol: 50°C for 2 minutes, 95°C for 10 minutes, then 40 cycles of (95°C for 15 seconds, 60°C for 1 minutes. Glyceraldehyde-3-phosphate dehydrogenase (GAPDH) acted as an internal positive control and sample of the bath solution was used as a no-template negative control, with all single-cell RT-PCR products expressing GAPDH, whilst bath control samples did not. The quantitative assessment of gene expression was determined by quantification of cycle (Cq) values lower than the threshold of 35 that were considered as positive. In total, 15 single cells per spinal region (TL) per mouse (n=3) were isolated, therefore the expression of mRNA transcripts was determined in 45 colonic sensory neurons.

Immunohistochemistry of Fast Blue-labelled colonic sensory neurons from *Mrgprd*^{EGFP} tagged mice.

From thoracolumbar regions, DRG T13 were stained from 4 *Mrgprd*^{EGFP} mice retrogradely labelled with Fast Blue to the colon, as described above. A single T13 DRG was sectioned sequentially across 10 slides at 12 µm thickness. Therefore, on a given slide, the T13 DRG was sampled at 120 µm intervals for the full thickness of the DRG. In total 16 sections from 4 animals were analysed, yielding 274 Fast Blue labelled cells. Slides were stained with chicken anti-GFP (1:1000; Abcam Ab13790) and rabbit anti-CGRP (1:10000, Sigma C8198) antisera. Secondary antibody used were goat anti-Chicken-488 (1:1000) and donkey anti-Rabbit-594 (1:1000). Each probe (e.g. *Mrgprd*^{EGFP} and CGRP) per section has a background reading subtracted and was normalised between the maximum and minimum intensity cells. A threshold of mean + 3 times SD for the minimum intensity cells (from all 16 sections) was used to differentiate positive from negative cells. Positive cells were then manually confirmed.

Ca^{2+} imaging of mouse sensory neurons

Dorsal root ganglia of wild-type and Mrgprd deficient mice were rinsed in cold HBSS (Invitrogen), and enzymatically dissociated as described previously (*63*). Neurons were plated in 96 wells plate (fluorescence Greiner bio one, Domique Dutscher, Brumath, France) and cultured for 24 hours. In a first set of experiments, neurons were treated with 5-oxoETE (1, 5, 25, 50 and 100 µM) or vehicle (HBSS). In a second set of experiments, neurons were incubated for 1 hour with 10 µg/mL of isolectin B4 from Griffonia simplicifolia conjugated to Alexa Fluor® 594 (ThermoFisher) in order to differentiate IB4-positive and -negative sensory neurons. Ca^{2+} flux was monitored by recording changing emission intensity of Fluo-4 (Molecular probe) following treatment with 5-oxoETE (10 µM) or its vehicle. In a third set of experiments, neurons were pre-incubated with pertussis toxin (PTX, 250 ng/mL) overnight or with the U73122 phospholipase C inhibitor (10 µM) 30 min, before treatment with 5-oxoETE (50 µM) or its vehicle.

Expression of shRNA directed against *Mrgprd* in sensory neurons

Lentiviral particles were produced as previously described (*64*). Briefly, HEK293T/17 cells were cultured according to supplier's recommendations (ATCC, USA). $1.7x10^7$ cells were seeded into a 175 cm^2 culture flask containing 30 mL of DMEM (Gibco, USA) and then incubated at 37°C 5% CO_2. In the next day, cells were transfected with a mixture of structural (psPAX2 and pMD2.G; Addgene, Cambridge, MA, USA) and transfer vectors (shRNA Mrgprd-RFP-CB or the control shRNA-RFP-CB; OriGene Technologies, Rockville, USA), by using the transfection reagent GeneJuice (Millipore, USA). Cells were incubated overnight at 37°C 5% CO_2, then the medium was replaced by 18 mL of OptiMEM (Gibco, USA). Cell culture supernatants were harvested 48 h later, cleared by centrifugation and filtration with a 0.45 μm syringe filter. Neurons plated in 96 wells plate coated with poly-L-ornithine/laminin and cultivated in Neurobasal medium supplemented with B27 and L-glutamine were transduced with 50 μL of lentivirus supernatant. Three days later, a transduction efficiency of 35 % was achieved and calcium flux assay was performed in response to 5-oxoETE (10 μM), as described above.

Ca^{2+} flux in CHO cells expressing Mrgprd

Mouse *Mrgprd*-expression plasmid (OriGene Technologies, Rockville, USA) was transfected into CHO cells using GeneJuice Transfection Reagent (1 μg of plasmid for 3 μL of GeneJuice). The cells were incubated in Ham's F12 Nutrient Mixture with 5% of FBS. G418 (Sigma) was used as the selection antibiotic. 50×10^3 cells/well in a 96 wells plate were incubated with fluo-8 loading solution (Fluo-8-AM; Invitrogen) according to manufacturer's instructions. The fluorescence was then measured at 530 nm on a microplate reader (NOVOstar; BMG Labtech) for 1 min. Five seconds after the beginning of calcium measures, 5-oxoETE (1, 10, 25, 50, 100

and 200 µM) or β-alanine (Sigma-Aldrich; 1 mM) was added. Data were collected and analyzed with the NOVOstar software.

Ca^{2+} imaging of human sensory neurons

Experiments were conducted following the opinion number 14-164 of the institutional review board (IRB00003888) of French institute of medical research and health. Three human DRG T11 (thoracic position 11) were supplied through the national human tissue resource center from the national disease resource interchange (NDRI). DRG were received unfixed in DMEM at 4°C. DRG were dissected, minced in HBSS and incubated in Papain (27µg/mL) (Sigma, Saint Quentin Fallavier, France) for 20 min at 37°C. After a wash with L-15 Wash Buffer [Leibovitz's L-15 Medium (Invitrogen), 10% FBS (Invitrogen)] and HBSS, DRG were incubated in HBSS containing 1 mg/mL of collagenase type IV (Worthington, Lakewood, NJ, USA) and 4 mg/mL of dispase II (Sigma). L-15 Wash buffer was added to neutralize enzymatic activities and the suspension was centrifuged at 1000 g for 5 min. The cycle of digestion was repeated 3 times 15 min. Neurons in the pellet were suspended in Neurobasal medium (Invitrogen) containing 2% B27, 2 mmol/L glutamine, 1% penicillin/streptomycin and 10 µM each of cytosine arabinoside, 5-Fluoro-2′-deoxyuridine (FUDR), Uridine (all from Sigma). The medium was changed every 3 days without cytosine arabinoside. Cells were plated in CC2 LabTek II (Nunc, Domique Dutscher, Brumath, France) for calcium signalling assay as described above in response to 5-oxoETE (0.1, 1 and 10 µM) and immunochemistry.

Immunofluorescence in human dorsal root ganglia

Experiments were conducted following the opinion number 12-074 of the institutional review board (IRB00003888) of French institute of medical research and health. Two human DRG T11 (thoracic position 11) were supplied through the national human tissue resource center from the

national disease resource interchange (NDRI). DRG were received unfixed and cryoprotected. DRG were cut into 20 µm sections on a cryostat (Leica CM1950, Nanterre, France), and mounted on Superfrost slides (Thermo Fisher Scientific, Villebonne-sur-Yvette, France). Cultured sensory neurons and slides were washed in phosphate buffered saline (PBS), 0.5% Triton X-100, and 1% bovine serum albumin (BSA) solution (Sigma, Saint-Quentin Fallavier, France) and incubated overnight at 4°C with the anti–Mrgprd (1:100, LS-A4123, LifeSpan Biosciences, Clinisciences, Nanterre, France) and anti-PGP9.5 (1:500, AB86808, Abcam). After washing, slides and cultured DRG were incubated with the appropriate secondary antibody conjugated with Alexa Fluor 488 or Alexa Fluor 555, washed, and mounted with ProLong Gold reagent containing DAPI (Molecular Probes). Images were acquired using Zeiss LSM-710 confocal microscopes (Carl Zeiss MicroImaging, Jena, Germany) with 20X objective in the inverted configuration.

Statistics

Data are presented as means ± standard error of the mean (SEM). Analyses were performed using GraphPad Prism 5.0 software (GraphPad, San Diego, CA). Comparisons between-groups were performed by Mann-Whitney test. Multiple comparisons within groups were performed by Kruskal-Wallis test, followed by Dunn's post-test. Statistical significance was accepted at $P < 0.05$.

Study approval

The study protocol for biopsies collection was approved by the local Ethic Committee (64/2004/O/Sper and EM14/2006/O) and conducted in accordance with the Declaration of Helsinki. Patients and HC gave written informed consent. Fixed and fresh Human DRG were supplied through the national human tissue resource center from the national disease resource

interchange (NDRI, reference: DCEN1 001). Experiments on human DRG were conducted following the opinion number 14-164 of the institutional review board (IRB00003888) of French institute of medical research and health. Animal experiments were conducted following the European union council directive 2010/63/EU. Animal Care and ethic Committee of US006/CREFE (CEEA-122) approved the whole study protocol (permit No. MP/01/64/09/12). Experiments conducted at the University of Glasgow were approved by the University's Ethical Review Process Applications Panel, and were performed in accordance with the European Community directive 86/609/EC and the United Kingdom Animals (Scientific Procedures) Act 1986.

Supplementary Materials

Fig. S1: Concentration of PUFA metabolites in biopsies of IBS patients

Fig. S2: Concentration of PUFA metabolites in biopsies of all IBS patients.

Fig. S3: 5-oxoETE does not induce somatic or visceral inflammation *in vivo*.

Fig. S4: Mrgprd immunoreactivity is observed in mouse colon

Fig. S5: Mrgprd immunoreactivity is not observed in colon of Mrgprd deficient mice.

References

1. F. Mearin, B. E. Lacy, L. Chang, W. D. Chey, A. J. Lembo, M. Simren, R. Spiller, Bowel Disorders. *Gastroenterology*, (2016).
2. P. Enck, Q. Aziz, G. Barbara, A. D. Farmer, S. Fukudo, E. A. Mayer, B. Niesler, E. M. Quigley, M. Rajilic-Stojanovic, M. Schemann, J. Schwille-Kiuntke, M. Simren, S. Zipfel, R. C. Spiller, Irritable bowel syndrome. *Nat Rev Dis Primers* **2**, 16014 (2016).
3. L. Ohman, M. Simren, Pathogenesis of IBS: role of inflammation, immunity and neuroimmune interactions. *Nat Rev Gastroenterol Hepatol* **7**, 163-173 (2010).
4. N. Cenac, T. Bautzova, P. Le Faouder, N. A. Veldhuis, D. P. Poole, C. Rolland, J. Bertrand, W. Liedtke, M. Dubourdeau, J. Bertrand-Michel, L. Zecchi, V. Stanghellini, N. W. Bunnett, G. Barbara, N. Vergnolle, Quantification and Potential Functions of Endogenous Agonists of Transient Receptor Potential Channels in Patients With Irritable Bowel Syndrome. *Gastroenterology* **149**, 433-444 e437 (2015).
5. G. Barbara, B. Wang, V. Stanghellini, G. R. De, C. Cremon, N. G. Di, M. Trevisani, B. Campi, P. Geppetti, M. Tonini, N. W. Bunnett, D. Grundy, R. Corinaldesi, Mast cell-dependent excitation of visceral-nociceptive sensory neurons in irritable bowel syndrome. *Gastroenterology* **132**, 26-37 (2007).
6. G. Clarke, S. M. O'Mahony, A. A. Hennessy, P. Ross, C. Stanton, J. F. Cryan, T. G. Dinan, Chain reactions: Early-life stress alters the metabolic profile of plasma polyunsaturated fatty acids in adulthood. *Behavioural Brain Research* **205**, 319-321 (2009).
7. G. Clarke, P. Fitzgerald, A. A. Hennessy, E. M. Cassidy, E. M. Quigley, P. Ross, C. Stanton, J. F. Cryan, T. G. Dinan, Marked elevations in pro-inflammatory polyunsaturated fatty acid metabolites in females with irritable bowel syndrome. *J.Lipid Res.* **51**, 1186-1192 (2010).
8. S. Tokuyama, K. Nakamoto, Unsaturated fatty acids and pain. *Biol Pharm Bull* **34**, 1174-1178 (2011).
9. A. A. Berbert, C. R. Kondo, C. L. Almendra, T. Matsuo, I. Dichi, Supplementation of fish oil and olive oil in patients with rheumatoid arthritis. *Nutrition* **21**, 131-136 (2005).
10. P. C. Calder, Session 3: Joint Nutrition Society and Irish Nutrition and Dietetic Institute Symposium on 'Nutrition and autoimmune disease' PUFA, inflammatory processes and rheumatoid arthritis. *Proc Nutr Soc* **67**, 409-418 (2008).
11. Z. Harel, F. M. Biro, R. K. Kottenhahn, S. L. Rosenthal, Supplementation with omega-3 polyunsaturated fatty acids in the management of dysmenorrhea in adolescents. *Am J Obstet Gynecol* **174**, 1335-1338 (1996).
12. A. Belluzzi, S. Boschi, C. Brignola, A. Munarini, G. Cariani, F. Miglio, Polyunsaturated fatty acids and inflammatory bowel disease. *Am J Clin Nutr* **71**, 339S-342S (2000).
13. D. Miyazawa, A. Ikemoto, Y. Fujii, H. Okuyama, Dietary alpha-linolenic acid suppresses the formation of lysophosphatidic acid, a lipid mediator, in rat platelets compared with linoleic acid. *Life Sci* **73**, 2083-2090 (2003).
14. C. Ramsden, C. Gagnon, J. Graciosa, K. Faurot, R. David, J. A. Bralley, R. N. Harden, Do omega-6 and trans fatty acids play a role in complex regional pain syndrome? A pilot study. *Pain Med* **11**, 1115-1125 (2010).
15. A. M. Patwardhan, P. E. Scotland, A. N. Akopian, K. M. Hargreaves, Activation of TRPV1 in the spinal cord by oxidized linoleic acid metabolites contributes to inflammatory hyperalgesia. *Proc Natl Acad Sci U S A* **106**, 18820-18824 (2009).
16. J. Y. Lim, C. K. Park, S. W. Hwang, Biological Roles of Resolvins and Related Substances in the Resolution of Pain. *Biomed Res Int* **2015**, 830930 (2015).
17. Z. Z. Xu, L. Zhang, T. Liu, J. Y. Park, T. Berta, R. Yang, C. N. Serhan, R. R. Ji, Resolvins RvE1 and RvD1 attenuate inflammatory pain via central and peripheral actions. *Nat Med* **16**, 592-597, 591p following 597 (2010).

18. S. Bang, S. Yoo, T. J. Yang, H. Cho, Y. G. Kim, S. W. Hwang, Resolvin D1 attenuates activation of sensory transient receptor potential channels leading to multiple anti-nociception. *Br J Pharmacol* **161**, 707-720 (2010).
19. C. K. Park, Z. Z. Xu, T. Liu, N. Lu, C. N. Serhan, R. R. Ji, Resolvin D2 is a potent endogenous inhibitor for transient receptor potential subtype V1/A1, inflammatory pain, and spinal cord synaptic plasticity in mice: distinct roles of resolvin D1, D2, and E1. *J Neurosci* **31**, 18433-18438 (2011).
20. C. K. Park, Maresin 1 Inhibits TRPV1 in Temporomandibular Joint-Related Trigeminal Nociceptive Neurons and TMJ Inflammation-Induced Synaptic Plasticity in the Trigeminal Nucleus. *Mediators Inflamm* **2015**, 275126 (2015).
21. H. Harizi, J. B. Corcuff, N. Gualde, Arachidonic-acid-derived eicosanoids: roles in biology and immunopathology. *Trends Mol.Med.* **14**, 461-469 (2008).
22. G. A. Higgs, S. Moncada, J. R. Vane, Eicosanoids in inflammation. *Ann Clin Res* **16**, 287-299 (1984).
23. L. W. Fu, J. C. Longhurst, Bradykinin and thromboxane A2 reciprocally interact to synergistically stimulate cardiac spinal afferents during myocardial ischemia. *Am J Physiol Heart Circ Physiol* **298**, H235-244 (2010).
24. J. C. Longhurst, R. A. Benham, S. V. Rendig, Increased concentration of leukotriene B4 but not thromboxane B2 in intestinal lymph of cats during brief ischemia. *Am J Physiol* **262**, H1482-1485 (1992).
25. S. Zhang, G. Grabauskas, X. Wu, M. K. Joo, A. Heldsinger, I. Song, C. Owyang, S. Yu, Role of prostaglandin D2 in mast cell activation-induced sensitization of esophageal vagal afferents. *Am J Physiol Gastrointest Liver Physiol* **304**, G908-916 (2013).
26. M. S. Gold, L. Zhang, D. L. Wrigley, R. J. Traub, Prostaglandin E(2) modulates TTX-R I(Na) in rat colonic sensory neurons. *J Neurophysiol* **88**, 1512-1522 (2002).
27. C. I. Svensson, M. Zattoni, C. N. Serhan, Lipoxins and aspirin-triggered lipoxin inhibit inflammatory pain processing. *J Exp Med* **204**, 245-252 (2007).
28. M. J. Zylka, F. L. Rice, D. J. Anderson, Topographically distinct epidermal nociceptive circuits revealed by axonal tracers targeted to Mrgprd. *Neuron* **45**, 17-25 (2005).
29. M. W. Buczynski, D. S. Dumlao, E. A. Dennis, Thematic Review Series: Proteomics. An integrated omics analysis of eicosanoid biology. *J Lipid Res* **50**, 1015-1038 (2009).
30. R. R. Ji, Z. Z. Xu, G. Strichartz, C. N. Serhan, Emerging roles of resolvins in the resolution of inflammation and pain. *Trends Neurosci* **34**, 599-609 (2011).
31. A. E. Barden, M. Moghaddami, E. Mas, M. Phillips, L. G. Cleland, T. A. Mori, Specialised pro-resolving mediators of inflammation in inflammatory arthritis. *Prostaglandins Leukot Essent Fatty Acids* **107**, 24-29 (2016).
32. W. S. Powell, J. Rokach, Biosynthesis, biological effects, and receptors of hydroxyeicosatetraenoic acids (HETEs) and oxoeicosatetraenoic acids (oxo-ETEs) derived from arachidonic acid. *Biochim Biophys Acta* **1851**, 340-355 (2015).
33. W. S. Powell, F. Gravelle, S. Gravel, Metabolism of 5(S)-hydroxy-6,8,11,14-eicosatetraenoic acid and other 5(S)-hydroxyeicosanoids by a specific dehydrogenase in human polymorphonuclear leukocytes. *J Biol Chem* **267**, 19233-19241 (1992).
34. W. S. Powell, F. Gravelle, S. Gravel, Phorbol myristate acetate stimulates the formation of 5-oxo-6,8,11,14-eicosatetraenoic acid by human neutrophils by activating NADPH oxidase. *J Biol Chem* **269**, 25373-25380 (1994).
35. Y. Zhang, A. Styhler, W. S. Powell, Synthesis of 5-oxo-6,8,11,14-eicosatetraenoic acid by human monocytes and lymphocytes. *J Leukoc Biol* **59**, 847-854 (1996).
36. U. Zimpfer, S. Dichmann, C. C. Termeer, J. C. Simon, J. M. Schroder, J. Norgauer, Human dendritic cells are a physiological source of the chemotactic arachidonic acid metabolite 5-oxo-eicosatetraenoic acid. *Inflamm Res* **49**, 633-638 (2000).

37. K. R. Erlemann, C. Cossette, S. Gravel, A. Lesimple, G. J. Lee, G. Saha, J. Rokach, W. S. Powell, Airway epithelial cells synthesize the lipid mediator 5-oxo-ETE in response to oxidative stress. *Free Radic Biol Med* **42**, 654-664 (2007).
38. P. B. Stamatiou, C. C. Chan, G. Monneret, D. Ethier, J. Rokach, W. S. Powell, 5-oxo-6,8,11,14-eicosatetraenoic acid stimulates the release of the eosinophil survival factor granulocyte/macrophage colony-stimulating factor from monocytes. *J Biol Chem* **279**, 28159-28164 (2004).
39. M. Guilbert, C. Ferland, M. Bosse, N. Flamand, S. Lavigne, M. Laviolette, 5-Oxo-6,8,11,14-eicosatetraenoic acid induces important eosinophil transmigration through basement membrane components: comparison of normal and asthmatic eosinophils. *Am J Respir Cell Mol Biol* **21**, 97-104 (1999).
40. G. E. Grant, J. Rokach, W. S. Powell, 5-Oxo-ETE and the OXE receptor. *Prostaglandins Other Lipid Mediat* **89**, 98-104 (2009).
41. E. Kocak, E. Akbal, S. Koklu, B. Ergul, M. Can, The Colonic Tissue Levels of TLR2, TLR4 and Nitric Oxide in Patients with Irritable Bowel Syndrome. *Intern Med* **55**, 1043-1048 (2016).
42. T. Shinohara, M. Harada, K. Ogi, M. Maruyama, R. Fujii, H. Tanaka, S. Fukusumi, H. Komatsu, M. Hosoya, Y. Noguchi, T. Watanabe, T. Moriya, Y. Itoh, S. Hinuma, Identification of a G protein-coupled receptor specifically responsive to beta-alanine. *J Biol Chem* **279**, 23559-23564 (2004).
43. D. J. Cavanaugh, H. Lee, L. Lo, S. D. Shields, M. J. Zylka, A. I. Basbaum, D. J. Anderson, Distinct subsets of unmyelinated primary sensory fibers mediate behavioral responses to noxious thermal and mechanical stimuli. *Proc Natl Acad Sci U S A* **106**, 9075-9080 (2009).
44. K. K. Rau, S. L. McIlwrath, H. Wang, J. J. Lawson, M. P. Jankowski, M. J. Zylka, D. J. Anderson, H. R. Koerber, Mrgprd enhances excitability in specific populations of cutaneous murine polymodal nociceptors. *J Neurosci* **29**, 8612-8619 (2009).
45. J. Zhang, D. J. Cavanaugh, M. I. Nemenov, A. I. Basbaum, The modality-specific contribution of peptidergic and non-peptidergic nociceptors is manifest at the level of dorsal horn nociresponsive neurons. *J Physiol* **591**, 1097-1110 (2013).
46. Q. Liu, P. Sikand, C. Ma, Z. Tang, L. Han, Z. Li, S. Sun, R. H. LaMotte, X. Dong, Mechanisms of itch evoked by beta-alanine. *J Neurosci* **32**, 14532-14537 (2012).
47. S. K. Ajit, M. H. Pausch, J. D. Kennedy, E. J. Kaftan, Development of a FLIPR assay for the simultaneous identification of MrgD agonists and antagonists from a single screen. *J Biomed Biotechnol* **2010**, (2010).
48. J. A. Christianson, R. J. Traub, B. M. Davis, Differences in spinal distribution and neurochemical phenotype of colonic afferents in mouse and rat. *J Comp Neurol* **494**, 246-259 (2006).
49. D. R. Robinson, P. A. McNaughton, M. L. Evans, G. A. Hicks, Characterization of the primary spinal afferent innervation of the mouse colon using retrograde labelling. *Neurogastroenterol Motil* **16**, 113-124 (2004).
50. J. R. Hockley, G. Boundouki, V. Cibert-Goton, C. McGuire, P. K. Yip, C. Chan, M. Tranter, J. N. Wood, M. A. Nassar, L. A. Blackshaw, Q. Aziz, G. J. Michael, M. D. Baker, W. J. Winchester, C. H. Knowles, D. C. Bulmer, Multiple roles for NaV1.9 in the activation of visceral afferents by noxious inflammatory, mechanical, and human disease-derived stimuli. *Pain* **155**, 1962-1975 (2014).
51. J. R. F. Hockley, T. S. Taylor, G. Callejo, A. L. Wilbrey, A. Gutteridge, K. Bach, W. J. Winchester, D. C. Bulmer, G. McMurray, E. S. J. Smith, Single-cell RNAseq reveals seven classes of colonic sensory neuron. *Gut*, (2018).
52. R. A. Crozier, S. K. Ajit, E. J. Kaftan, M. H. Pausch, MrgD activation inhibits KCNQ/M-currents and contributes to enhanced neuronal excitability. *J Neurosci* **27**, 4492-4496 (2007).
53. G. Blackburn-Munro, B. S. Jensen, The anticonvulsant retigabine attenuates nociceptive behaviours in rat models of persistent and neuropathic pain. *Eur J Pharmacol* **460**, 109-116 (2003).

54. G. M. Passmore, A. A. Selyanko, M. Mistry, M. Al-Qatari, S. J. Marsh, E. A. Matthews, A. H. Dickenson, T. A. Brown, S. A. Burbidge, M. Main, D. A. Brown, KCNQ/M currents in sensory neurons: significance for pain therapy. *J Neurosci* **23**, 7227-7236 (2003).
55. K. Hirano, K. Kuratani, M. Fujiyoshi, N. Tashiro, E. Hayashi, M. Kinoshita, Kv7.2-7.5 voltage-gated potassium channel (KCNQ2-5) opener, retigabine, reduces capsaicin-induced visceral pain in mice. *Neurosci Lett* **413**, 159-162 (2007).
56. M. Peiris, J. R. Hockley, D. E. Reed, E. S. J. Smith, D. C. Bulmer, L. A. Blackshaw, Peripheral KV7 channels regulate visceral sensory function in mouse and human colon. *Mol Pain* **13**, 1744806917709371 (2017).
57. P. Le Faouder, V. Baillif, I. Spreadbury, J. P. Motta, P. Rousset, G. Chene, C. Guigne, F. Terce, S. Vanner, N. Vergnolle, J. Bertrand-Michel, M. Dubourdeau, N. Cenac, LC-MS/MS method for rapid and concomitant quantification of pro-inflammatory and pro-resolving polyunsaturated fatty acid metabolites. *J Chromatogr B Analyt Technol Biomed Life Sci* **932**, 123-133 (2013).
58. H. Wang, M. J. Zylka, Mrgprd-expressing polymodal nociceptive neurons innervate most known classes of substantia gelatinosa neurons. *J Neurosci* **29**, 13202-13209 (2009).
59. L. Basso, J. Boue, K. Mahiddine, C. Blanpied, S. Robiou-du-Pont, N. Vergnolle, C. Deraison, G. Dietrich, Endogenous analgesia mediated by CD4(+) T lymphocytes is dependent on enkephalins in mice. *J Neuroinflammation* **13**, 132 (2016).
60. J. Boue, L. Basso, N. Cenac, C. Blanpied, M. Rolli-Derkinderen, M. Neunlist, N. Vergnolle, G. Dietrich, Endogenous regulation of visceral pain via production of opioids by colitogenic CD4(+) T cells in mice. *Gastroenterology* **146**, 166-175 (2014).
61. S. M. Brierley, R. C. Jones, 3rd, G. F. Gebhart, L. A. Blackshaw, Splanchnic and pelvic mechanosensory afferents signal different qualities of colonic stimuli in mice. *Gastroenterology* **127**, 166-178 (2004).
62. J. R. Hockley, M. M. Tranter, C. McGuire, G. Boundouki, V. Cibert-Goton, M. A. Thaha, L. A. Blackshaw, G. J. Michael, M. D. Baker, C. H. Knowles, W. J. Winchester, D. C. Bulmer, P2Y Receptors Sensitize Mouse and Human Colonic Nociceptors. *J Neurosci* **36**, 2364-2376 (2016).
63. N. Cenac, M. Castro, C. Desormeaux, P. Colin, M. Sie, M. Ranger, N. Vergnolle, A novel orally administered trimebutine compound (GIC-1001) is anti-nociceptive and features peripheral opioid agonistic activity and Hydrogen Sulphide-releasing capacity in mice. *Eur J Pain* **20**, 723-730 (2016).
64. A. Denadai-Souza, C. M. Ribeiro, C. Rolland, A. Thouard, C. Deraison, C. Scavone, D. Gonzalez-Dunia, N. Vergnolle, M. C. W. Avellar, Effect of tryptase inhibition on joint inflammation: a pharmacological and lentivirus-mediated gene transfer study. *Arthritis Res Ther* **19**, 124 (2017).

Acknowledgments: The authors thank the microscope core facility, INSERM UMR1043, Toulouse, the animal care facility, Genetoul, anexplo, US006/INSERM, Toulouse and the animal experiment platform of Toxalim (Research Centre in Food Toxicology), Toulouse University, INRA, ENVT, INP-Purpan, UPS, Toulouse, for their technical support. The authors acknowledge the National Diseases Research Interchange (NDRI) for supplying the human DRG. Lipidomic analyses were performed on the Toulouse INSERM Metatoul-Lipidomique Core Facility-MetaboHub ANR-11-INBS-010. Mrgprd deficient mice were a generous gift from David J Anderson (Caltech). **Funding:** Alexandre Denadai-Souza was recipient of a post-doctoral fellowship from São Paulo Research Foundation (FAPESP; process 2012/07784-4). Giovanni Barbara is a recipient of an educational grant from Fondazione del Monte di Bologna e Ravenna, Bologna, Italy. This work was supported by the Agence Nationale de la Recherche (to Nicolas Cenac), the Region Midi-Pyrénées (to Pauline Le Faouder and Nicolas Cenac), the Italian Ministry of Education, University and Research (No. 2002052573 and No. 2007Z292XF and 2009MFSXNZ) and funds from the University of Bologna (to Giovanni Barbara), funds from Bowel and Cancer Research (to Michael M. Tranter), BBSRC (BB/P007996/1 to David I Hughes, and BB/R006210/1 to James R F Hockley and Ewan St John Smith), a Rosetrees Postdoctoral Grant (A1296) awarded to James R F Hockley and Ewan St John Smith, and a European Research Council (ERC) grant to Nathalie Vergnolle (ERC-2012-StG-20111109). This work was also supported by the platform Aninfimip, an EquipEx (‘Equipement d’Excellence’) supported by the French government through the Investments for the Future program (ANR-11-EQPX-0003). **Author contributions:** TB, TPB and JRFH: design research studies, conduct experiments, acquire and analyze data. MMT, MRB, PLF, JP and CD: acquire and analyze data. LB, CR and ADS: conduct experiments. AM, PM and DIH: raised the different genetically modified mice and participate to the revision of the manuscript. EJS: participate to the revision of the manuscript. NV, AM, HE and GD: write the manuscript. GB: conduct experiments and write the manuscript. DB: conduct experiments, analyze data and write the manuscript. NC: design research studies, conduct experiments, acquire data, analyze data and write the manuscript. **Competing interests:** The authors have declared that no conflict of interest exists.

Table 1: Characteristics of patients from which biopsies were collected for PUFA metabolites quantification

	Control	IBS
Number	14	50
Age	49 (20-76)	43 (20-72)
Sex ratio (F/M)	8/6	32/18
Bowel movements:		
Diarrhea	0	20
Constipation	0	20
Mix	0	10

Table 2: Percentage of fast-blue positive neurons expressing Mrgprd, CGRP or both per Mrgprd-GFP mouse DRG T13

Animal	Mrgprd+	CGRP+	Mrgprd+ & CGRP+
A	9 / 75 (12.0%)	54 / 75 (72.0%)	0 / 75 (0.0%)
B	2 / 38 (5.3%)	24 / 38 (63.2%)	0 / 38 (0.0%)
C	10 / 101 (9.9%)	64 / 101 (63.4%)	1 / 101 (1.0%)
D	1 / 60 (1.7%)	46 / 60 (76.7%)	0 / 60 (0.0%)
Total (mean ± SD)	7.2 ± 4.6 %	68.8 ± 6.7 %	0.3 ± 0.5 %

Figure 1

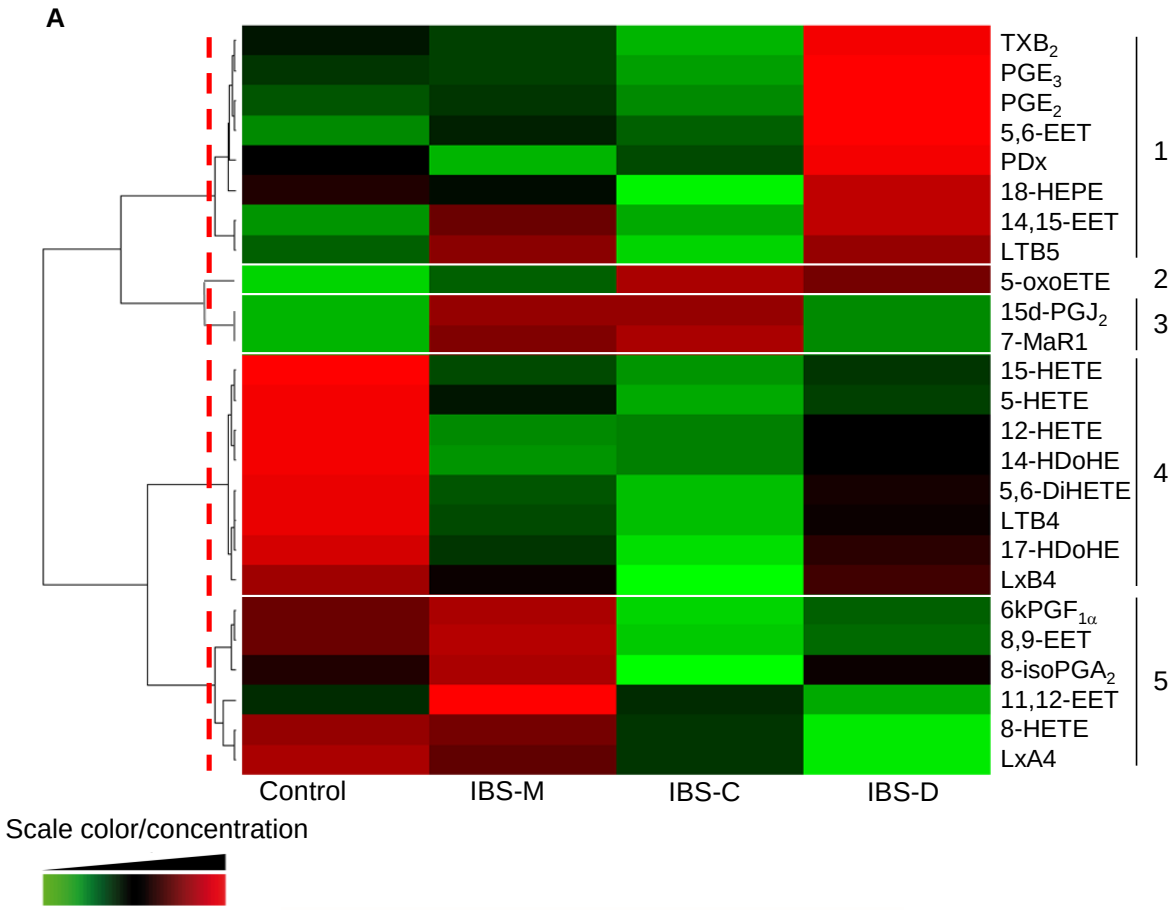

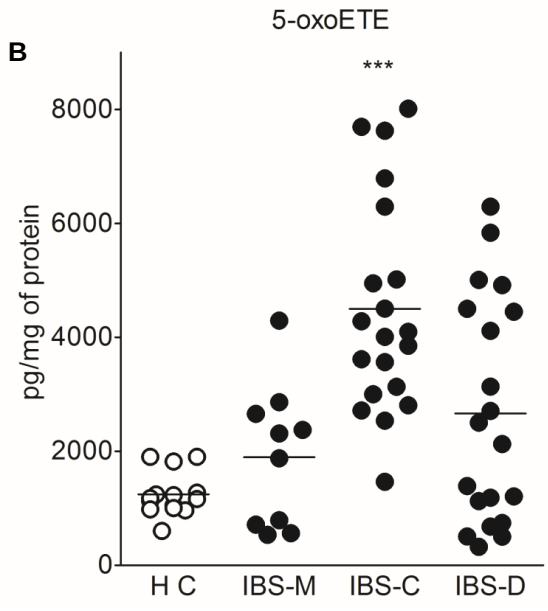

Fig.1: Quantification of PUFA metabolites in mucosa of IBS patients. A Heat-map of PUFA metabolites quantified by liquid chromatography-tandem mass spectrometry. Data are shown in a matrix format: each row represents a single PUFA metabolite, and each column represents

a subgroup of patients. Each color patch represents the normalized quantity of PUFA metabolites (row) in a subgroup of patients (column), with a continuum of quantity from bright green (lowest) to bright red (highest). The pattern and length of the branches in the dendrograms reflect the relatedness of the PUFA metabolites. The dashed red line is the dendrogram distance used to cluster PUFA metabolites. **B** 5-oxoETE quantified by liquid chromatography-tandem mass spectrometry in mucosa of healthy control (white circle) and IBS (black circle). Data are expressed in pg/mg protein and represented as mean ± SEM of 10 to 20 biopsies per group. Statistical analysis was performed using Kruskal-Wallis analysis of variance and subsequent Dunn's post hoc test. *** $p < 0.001$, significantly different from healthy control group.

Figure 2

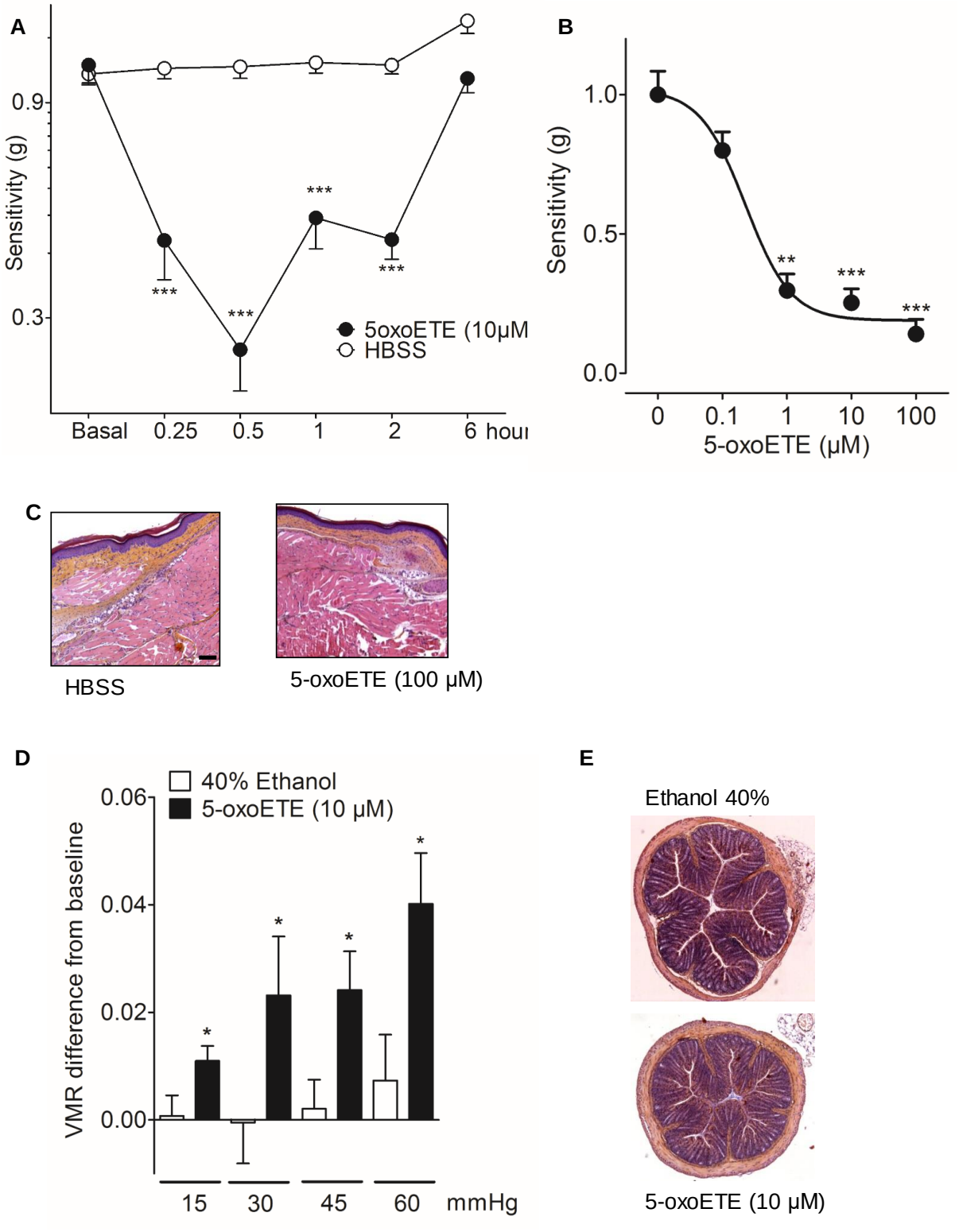

873

874 **Fig.2: 5-oxoETE induces somatic and visceral hypersensitivity *in vivo***. Mice were

875 subcutaneously injected with either HBSS (white circle) or 5-oxoETE (black circle) into hind

876 footpads. **A** Somatic pain monitored using the von Frey test at different times (15 and 30 min,

1, 2 and 6 hours) following 5-oxoETE (10 µM) injection; n=3 independent experiments of 5 mice per groups. **B** Von Frey test performed 30 min after injection of 5-oxoETE at different concentrations (0.1, 1, 10 or 100 µM); n=2 experiments of 6 mice per group. Data are expressed as mean ± SEM. **C** Mouse paw tissue samples stained with H&E 6 h after administration of HBSS (left panel) or 5-oxoETE (100 µM) (right panel). **D** Visceromotor response (VMR) to increasing pressures of colorectal distension before and 30 min after intracolonic administration of 5-oxoETE (10µM; black bars) or vehicle (40% ethanol; white bars); n=2 experiments of 10 mice per group. Data are expressed as mean ± SEM relative to the baseline recorded before treatment. **E** Colon tissue samples stained with H&E from 40% ethanol treated-mice (1 hour) (upper panel) or 5-oxoETE-treated mice (10 µM; 1 hour) (lower panel). Statistical analysis was performed using Kruskal-Wallis analysis of variance and subsequent Dunn's post hoc test. ** $p<0.01$, *** $p<0.001$, significantly different from control mice.

Figure 3

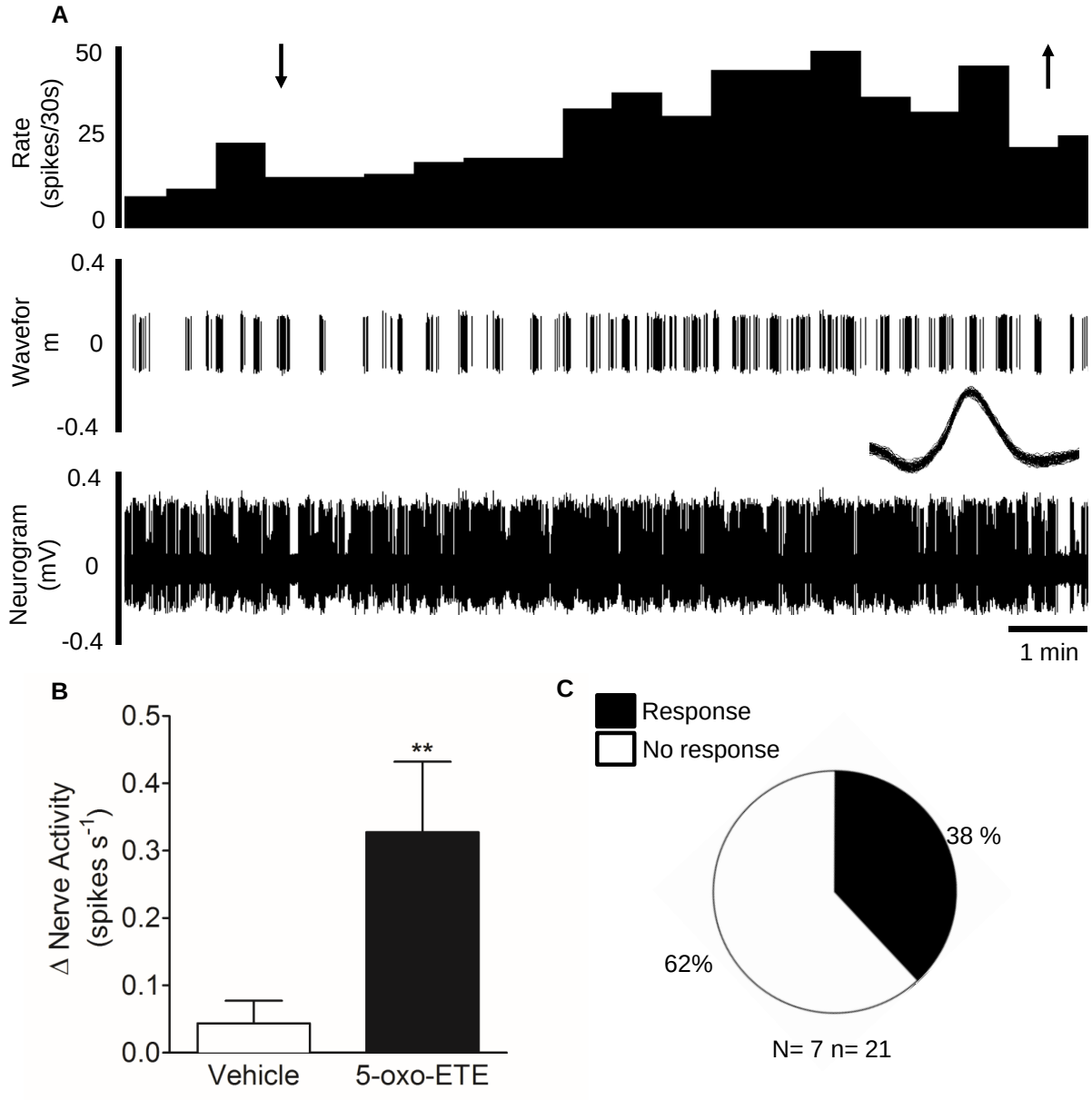

Fig.3: 5-oxoETE induces lumbar splanchnic nerve firing. A Example of multi-unit recording showing lumbar splanchnic (i.e. colon-innervating) nerve response to ring application (7 min) of 5-oxoETE in mouse serosal afferents. Arrows indicate application and removal of 5-oxoETE. **B** Mean change in firing/second in serosal and mesenteric receptive fields compared with vehicle response of Krebs buffer. Statistical analysis was performed using Mann-Whitney t-test. ** $p<0.01$, significantly different from vehicle. **C** Proportion of responses in lumbar splanchnic afferents to application of 5-oxoETE.

Figure 4

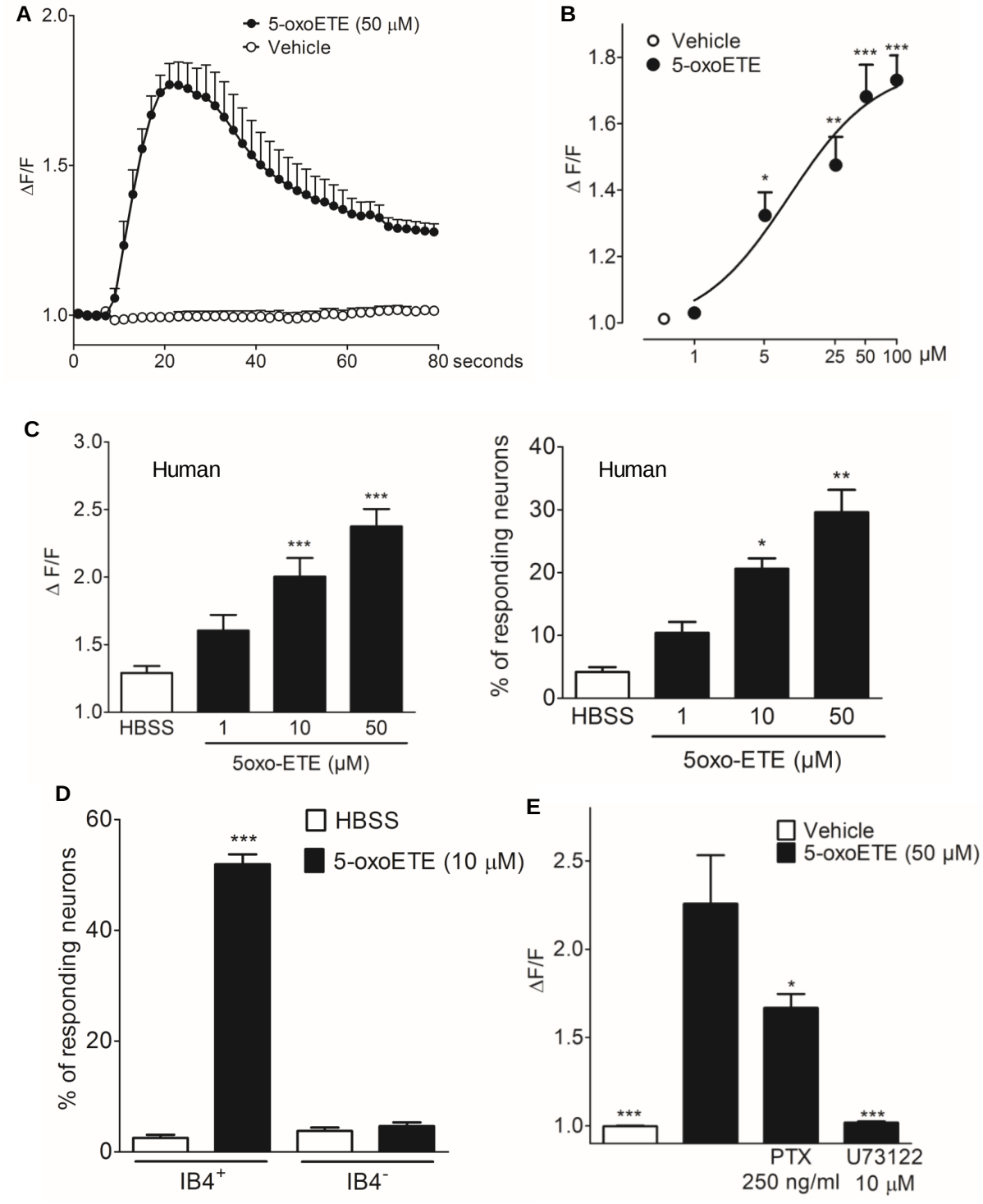

Fig.4: 5-oxoETE induces an increase in [Ca^{2+}] in sensory neurons via a GPCR. A Representative trace of Ca^{2+} flux experiments in sensory neurons performed without Ca^{2+}/Mg^{2+} in the extracellular medium and exposed to 5-oxoETE (50 μM) or its vehicle (HBSS). **B** Ca^{2+} flux in mouse sensory neurons exposed to increasing amounts of 5-oxoETE (black circle) or

vehicle (HBSS; white circle); n=7 independent experiments of 3 wells per condition and 60 to 80 neurons per well. **C** Amplitude of $[Ca^{2+}]_i$ (ΔF/F; left panel) in human sensory neurons and percentage of responding neurons (right panel) exposed to increasing amounts of 5-oxoETE (black bar) or vehicle (HBSS; white bar); n=3 independent experiments of 3 wells per condition and 20-53 neurons per well. **D** Percentage of isolectin B4-positive ($IB4^+$) and -negative ($IB4^-$) mouse sensory neurons responding to 10 µM of 5-oxoETE; n=3 independent experiments of 3 wells per condition and 60 to 80 neurons per well. **E** Effects of 30 min incubation with PLC inhibitor (U73122; 10 µM) or overnight incubation with pertussis toxin (PTX; 250 ng/ml) on 5-oxoETE-induced Ca^{2+} mobilization in mouse sensory neurons; n=5 independent experiments of 3 wells per condition and 60 to 80 neurons per well. Statistical analysis was performed using Kruskal-Wallis analysis of variance and subsequent Dunn's post hoc test. Data are mean ± SEM. * $p<0.05$, ** $p<0.01$, *** $p<0.001$ significantly different from HBSS group.

Figure 5

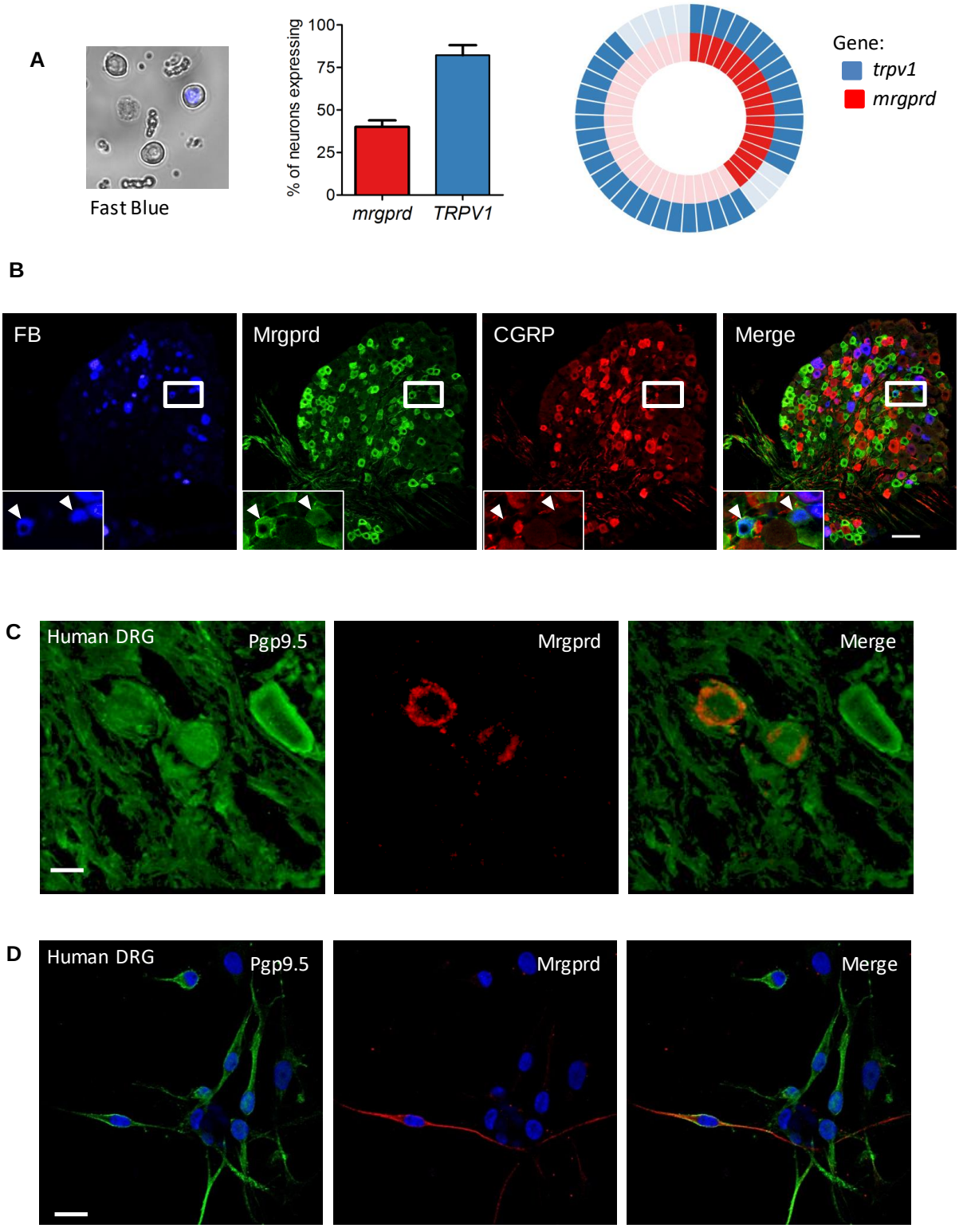

Fig.5: Expression of Mrgprd in sensory neurons. A Expression of *Mrgprd* (in red) and *trpv1* (in blue) mRNA transcripts by single-cell qRT-PCR (middle panel) of retrogradely labelled mouse colonic sensory neurons (left panel). Pie charts representation of the expression (dark

color) or not (light color) of *Mrgprd* and *Trpv1* mRNA in FB positive neurons (right panel), each segment represents a single colonic sensory neuron. **(B)** Representative images of GFP (green), CGRP- (red) immunoreactivity and FB labelling (blue) in a T13 DRG from *Mrgprd*^{EGFP} mouse where FB was injected into the colon (scale bar = 50 µm). Expression of Mrgprd in whole human dorsal root ganglia (**C**) and in primary culture of human sensory neurons (**D**); human whole DRG T11 (**C**, scale bar = 10 µm) or primary culture of sensory neurons (**D**, scale bar = 10 µm).

Figure 6

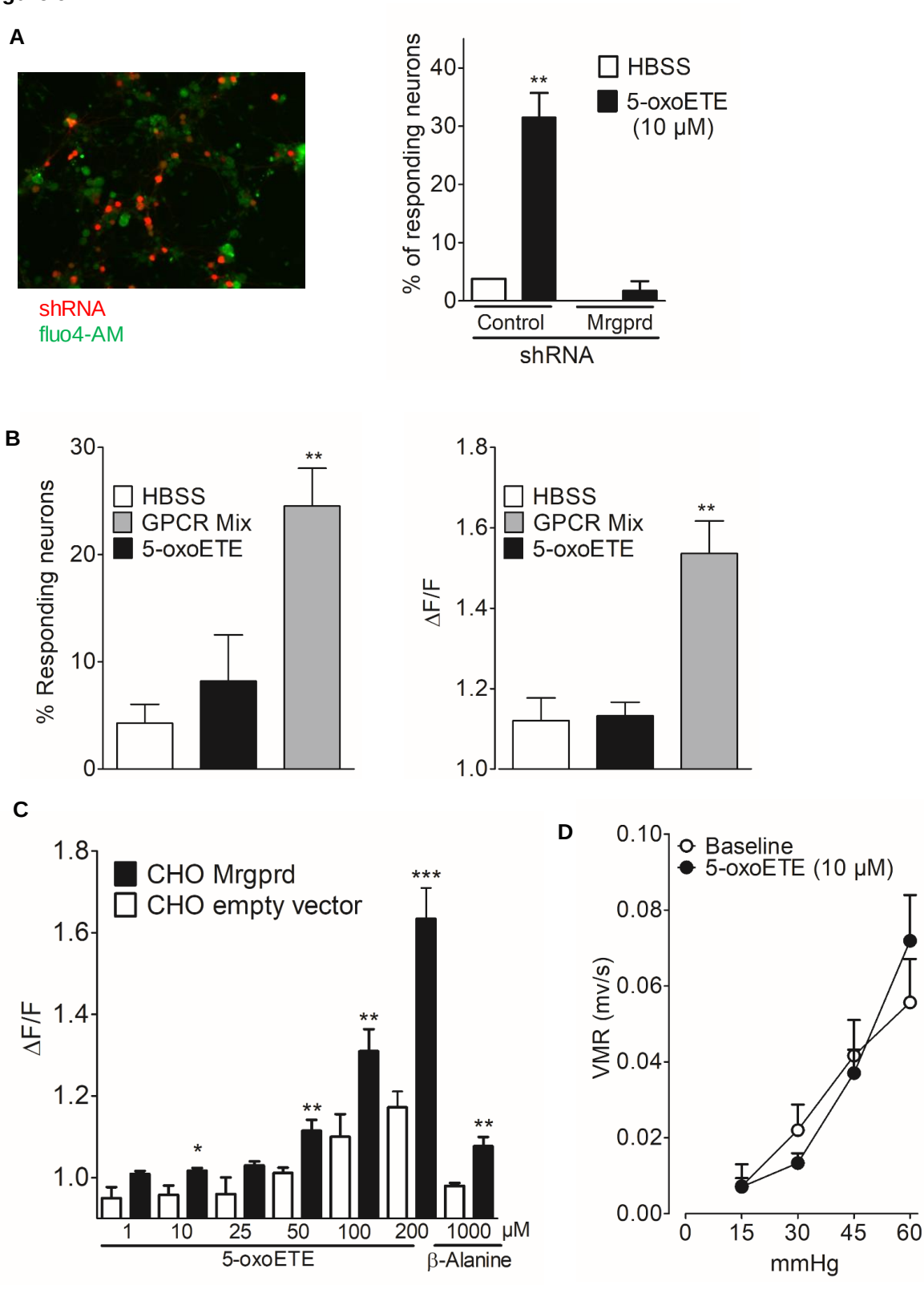

Fig.6: Mrgprd expression is required for the intracellular calcium mobilization and hypersensitivity induced by 5-oxoETE. A Left panel, representative picture of sensory neurons transfected with shRNA (in red) containing the calcium probe Fluo4 (in green); right

panel, percentage of shRNA directed against *Mrgprd* or control positive sensory neurons responding to 10 µM of 5-oxoETE; n=6 independent experiments of 3 wells per conditions and 10 to 32 analyzed neurons per well. **B** Percentage of responding neurons (right panel) and amplitude of intracellular calcium mobilization (ΔF/F; left panel) in mouse sensory neurons from Mrgprd deficient mice exposed to vehicle (HBSS; white bar), 5-oxoETE (10 µM, black bar) or to a mix of GPCR agonist (GPCR Mix: bradykinin, serotonin and histamine, 10 µM each; gray bar); n=4 independent experiments of 3 wells per condition and 20-50 neurons per well. **C** Effects of 5-oxoETE (1–200 µM) and β-Alanine (positive control), 1 mM) on the amplitude (ΔF/F) of calcium mobilization in HEK cells transiently expressing Mrgprd or vector control; n=8 independent experiments of 3 wells per condition. **D** Visceromotor response (VMR) in Mrgprd deficient mice to increasing pressures of colorectal distension before (baseline; white circle) and 30 min after intracolonic administration of 5-oxoETE (10 µM; black circle); n=2 experiments of 7 mice. Data are mean ± SEM. Statistical analysis was performed using Kruskal-Wallis analysis of variance and subsequent Dunn's post hoc test. ** $p<0.01$ significantly different from control shRNA/HBSS group (**A**); **$p<0.01$ significantly different from HBSS group **(B)**; * $p<0.05$; **$p<0.01$; *** $p<0.001$ significantly different from the corresponding CHO empty vector group (**C**).